

Aerosol non-sea-salt sulfate in the remote marine boundary layer under clear-sky and normal cloudiness conditions: Ocean-derived biogenic alkalinity enhances sea-salt sulfate production by ozone oxidation

H. Sievering

Department of Geography and Environmental Science, University of Colorado, Denver, Colorado, USA

Long-Term Ecological Research Program, Institute of Arctic and Alpine Research (INSTAAR), University of Colorado, Boulder, Colorado, USA

J. Cainey,¹ M. Harvey, J. McGregor, and S. Nichol

National Institute of Water and Atmospheric Research, Wellington, New Zealand

P. Quinn

Pacific Marine Environment Laboratory, National Oceanic and Atmospheric Administration, Seattle, Washington, USA

Received 1 November 2003; revised 2 June 2004; accepted 7 July 2004; published 14 October 2004.

[1] Observations of remote marine boundary layer (RMBL) non-sea-salt sulfate (NSS) aerosols indicate a substantial NSS fraction may be found in coarse (supermicron diameter) sea-salt aerosols. Aqueous phase mechanisms account for a portion of this coarse aerosol NSS. Aerosol samples were collected at Baring Head, New Zealand, during clear-sky and normal cloudiness conditions to assess the contribution that the O₃ oxidation mechanism may make to coarse NSS. Southern Ocean derived clear-sky coarse aerosols had >8 nmol NSS m⁻³; the normal cloudiness coarse aerosols contained <3 nmol NSS m⁻³. Data were obtained during high wind speeds ($U \sim 11 \text{ m s}^{-1}$), minimizing coarse aerosol lifetimes and thus cloud interaction. Both clear-sky and normal cloudiness coarse aerosols contained Ca excesses that contributed >200 and 35–40 times, respectively, more alkalinity than did bulk seawater (equivalents basis). Consequently, aqueous phase, O₃ oxidation in sea-salt aerosols was markedly enhanced and may account for essentially all observed coarse aerosol NSS. Satellite data indicate the Southern Ocean upwind of Baring Head contains ~3 times the annual primary productivity (with associated biogenic Ca enhancement) of open ocean surface waters. The large and variable upwind biogenic Ca source plus the high wind speeds encountered at Baring Head make this site atypical of many RMBL regions. More typical RMBL conditions, found during western Pacific Ocean shipboard measurements, indicate that ~1 to ~2.5 times additional alkalinity (beyond that from bulk seawater) is likely to be found in sea-salt aerosols due to seawater biogenic sources. Coarse aerosols, laden with NSS, experience large dry deposition rates which results in rapid recycling of ocean-derived sulfur. This process has been overlooked or understated in RMBL sulfur budget analyses and models. One major consequence is that new particle production from biogenically derived oceanic sulfur is severely limited in the RMBL since ubiquitous O₃ oxidation in sea-salt aerosols is energetically favored over homogeneous nucleation. *INDEX TERMS*: 0312 Atmospheric Composition and Structure: Air/sea constituent fluxes (3339, 4504); 0315 Atmospheric Composition and Structure: Biosphere/atmosphere interactions; 0305 Atmospheric Composition and Structure: Aerosols and particles (0345, 4801); 1615 Global Change: Biogeochemical processes (4805); *KEYWORDS*: sea-salt aerosols, alkalinity, biosphere-atmosphere interactions, sulfate, ozone, marine boundary layer

Citation: Sievering, H., J. Cainey, M. Harvey, J. McGregor, S. Nichol, and P. Quinn (2004), Aerosol non-sea-salt sulfate in the remote marine boundary layer under clear-sky and normal cloudiness conditions: Ocean-derived biogenic alkalinity enhances sea-salt sulfate production by ozone oxidation, *J. Geophys. Res.*, 109, D19317, doi:10.1029/2003JD004315.

¹Now at Cape Grim Baseline Air Pollution Station, Tasmania, Australia.

1. Introduction

[2] Observations of the size distribution of non-sea-salt sulfate (NSS) in the remote marine boundary layer (RMBL) have shown that a substantial fraction is found in $>1 \mu\text{m}$ ambient aerodynamic diameter, predominantly sea-salt aerosols [Gravenhorst, 1978; Sievering *et al.*, 1990; Prospero and Savoie, 1993]. Models used to predict the formation of sulfate over the global oceans often underestimate sulfate concentrations while markedly overestimating surface SO₂ concentrations [Barrie *et al.*, 2001; Kasibhatla *et al.*, 1997]. These supermicron or, simply, coarse aerosols have high dry deposition rates making removal of NSS to the ocean's surface waters an important consideration in MBL sulfur budgets. The percentage of total aerosol NSS that is found in coarse aerosols has been observed to be as little as 5% (polluted conditions) to as much as 50% (unpolluted conditions) in the MBL over the North Atlantic Ocean [Sievering *et al.*, 1991, 1995]. High wind speed conditions, supporting the substantial production of sea-salt aerosols, generally enhance this percentage [Sievering *et al.*, 1991, 1992].

[3] Modeling of the MBL sulfur cycle [e.g., Chameides and Stelson, 1992; von Glasow *et al.*, 2002] shows that multiphase SO₂ conversion in the high pH water associated with sea-salt aerosols, hereafter referred to as sea-salt aerosol water, can explain the large majority of observed coarse aerosol NSS. The RMBL contains SO₂ largely due to dimethylsulfide (DMS) emissions from the ocean's surface waters. The uptake of SO₂ and subsequent conversion of aqueous phase sulfur, S (IV), to NSS is understood to be fostered by three main oxidation pathways: by halogen chemistry [Vogt *et al.*, 1996; Keene *et al.*, 1998]; by ozone (O₃) oxidation [Sievering *et al.*, 1990, 1991, 1992]; and by hydrogen peroxide (H₂O₂) oxidation [Chameides and Stelson, 1992]. The H₂O₂ pathway is significant only after O₃ oxidation has caused a drop in the pH of sea-salt aerosol water [Sievering *et al.*, 1992]. The initial high pH of sea-salt aerosol water supports the rapid oxidation of S(IV) to NSS by O₃ oxidation but this process may be quenched once the bulk seawater-derived alkalinity in sea-salt aerosol water, given by $0.005 [\text{Na}^+]$ [Millero, 1974], is consumed and the pH drops off substantially [Chameides and Stelson, 1992; Sievering *et al.*, 1992]. Cloud production/processing may also contribute to coarse aerosol NSS, although far less so than in submicron aerosols [e.g., Gurciullo *et al.*, 1999]. This cloud NSS production/processing was also found to be a very minor contributor to total coarse aerosol NSS in the Southern Ocean RMBL during the first Aerosol Characterization Experiment (ACE-1) [Gurciullo *et al.*, 1999]. The results from this work in the Southern Ocean RMBL suggest cloud production/processing may be a contributor of lesser importance to coarse aerosol NSS in other ocean RMBL settings as well. Further, it was found that the actual alkalinity of sea-salt aerosol water was enhanced beyond its bulk seawater-derived alkalinity [Sievering *et al.*, 1999].

[4] Understanding of the global sulfur cycle must include quantitative assessment of multiphase SO₂ conversion in the RMBL. The Baring Head site, on the southern tip of New Zealand's North Island, provides a setting in which multiphase sulfur conversion in sea-salt aerosol water may be studied, on some occasions, with

essentially no contribution from cloud production/processing. Minimal cloud cover conditions may occur under certain synoptic conditions when the South Island of New Zealand acts as an effective cloud barrier. Clear-sky sea-salt aerosol trajectories to Baring Head may, then, result. Given that the average Baring Head southerly flow wind speed is over 10 m s^{-1} , the lifetime of coarse sea-salt aerosols is, generally, <1 to, at most, 2 days. Thus, for certain sampling periods of opportunity, coarse sea-salt aerosols will not have come in contact with clouds during their 0.5-day to 2-day lifetimes.

[5] Conditions conducive to the consideration of multiphase SO₂ conversion in the RMBL, without the influence of clouds, were obtained during an extended 27-month Baring Head field sampling campaign. The purpose of this paper is to (1) discuss and compare the size distribution of NSS and other ion data under clear-sky as well as normal cloudiness Southern Ocean RMBL sampling conditions, (2) estimate the contribution that O₃ oxidation in sea-salt aerosol water made to observed Southern Ocean RMBL aerosol NSS as well as estimate the portion of this NSS resulting from biogenically derived alkalinity enhancement of sea-salt aerosol water, and (3) assess the contribution that the O₃ oxidation pathway may make to observed open ocean marine boundary layer aerosol NSS.

2. Experiment

2.1. Site Description

[6] Atmospheric sampling was conducted at Baring Head, New Zealand ($41^\circ 24'S$, $174^\circ 52'E$) throughout years 2000, 2001 and into 2002. The site is maintained by the National Institute for Water and Atmospheric Research (NIWA) of New Zealand. Meteorological and ancillary aerosol sampling equipment is operated by NIWA. Baring Head, during southerly wind conditions, is ideally located to sample oceanic air masses that have experienced no recent contact with land and that may have experienced high wind speeds. However, wind trajectories encountered at Baring Head are predominantly northwesterly, with periodic southerly or southwesterly flow for about one fourth of the time during which very clean marine air is brought to the site. A 12-m sampling tower at the edge of a sloping cliff is designed to reduce the collection of aerosols derived from the surf zone, the narrow beach, or the cliff face during southerly airflow conditions. Previous aerosol chemical analysis data, collected under southerly airflow conditions [Allen *et al.*, 1997; NIWA, unpublished data, 2002] have shown that a minimal soil contribution to aerosol sampling may be derived from the cliff face under $>9 \text{ m s}^{-1}$ wind speed conditions. Flow, for other than southerly flow sampling conditions, may introduce a very minor amount of pollution. However, the surrounding area is predominantly grass covered and is only occasionally used for sheep and cattle grazing, making local contamination insignificant [Allen *et al.*, 1997].

2.2. Sample Collection

[7] A six-stage high-volume (1130 lpm) cascade impactor (Graseby-Anderson), which efficiently samples 0.1 to $16 \mu\text{m}$ diameter ambient aerosols, was installed at the top of the

Table 1. Coarse, Fine, and Very Fine Aerosol Ion Concentrations Found During Normal Southerly and Clear Sky Southerly Sampling During 2000–2002^a

Diameter, μm	Na ⁺	Mg ⁺⁺	Alk	Ca ⁺⁺	SO ₄ ⁼	Sea SO ₄	NO ₃ ⁻	CaX	K ⁺	Soil SO ₄	Ca ⁺⁺ Excess	NSS(Mg)
<i>Normal Southerly</i>												
0.9–16 (Coarse)	145.8 (± 58.0)	7.25 (± 2.9)	0.32 (± 0.13)	14.7 (± 5.8)	8.3 (± 3.8)	3.9 (± 1.5)	1.32 (± 0.84)	13.3 (± 5.8)	4.4 (± 1.8)	1.8 (± 0.7)	6.0 (± 6.0)	2.6 (± 1.1)
0.4–0.9 (Fine)	6.62 (± 4.96)	0.23 (± 0.18)	0.01 (± 0.01)	1.06 (± 0.86)	0.6 (± 0.3)	0.12 (± 0.10)	0.15 (± 0.10)	0.56 (± 0.43)	0.32 (± 0.31)	0.13 (± 0.13)	0.03 (± 0.03)	0.4 (± 0.2)
<0.4 (Very Fine)	2.77 (± 2.61)	0.07 (± 0.01)	0	0.30 (± 0.24)	0.8 (± 0.2)	0.04 (± 0.04)	0.11 (± 0.08)	0.16 (± 0.18)	0.17 (± 0.18)	0.07 (± 0.08)	0	0.7 (± 0.3)
<i>Clear Sky Southerly</i>												
0.9–16 (Coarse)	157.2 (± 56.2)	5.16 (± 1.90)	0.23 (± 0.09)	36.4 (± 14.5)	12.5 (± 5.4)	2.7 (± 1.0)	3.6 (± 1.7)	35.4 (± 14.5)	3.3 (± 1.3)	1.4 (± 0.7)	30.0 (± 18.5)	8.4 (± 3.1)
0.4–0.9 (Fine)	16.6 (± 13.8)	0.51 (± 0.39)	0.02 (± 0.02)	3.49 (± 2.52)	1.6 (± 1.1)	0.27 (± 0.26)	0.79 (± 0.71)	3.4 (± 2.3)	0.6 (± 0.6)	0.3 (± 0.4)	2.5 (± 2.4)	1.1 (± 0.5)
<0.4 (Very Fine)	5.72 (± 3.43)	0.28 (± 0.19)	0.01 (± 0.01)	3.45 (± 3.22)	3.0 (± 1.4)	0.15 (± 0.10)	0.57 (± 0.51)	3.4 (± 2.8)	0.8 (± 0.8)	0.4 (± 0.4)	2.1 (± 2.1)	2.2 (± 0.9)

^aNormal southerly refers to samples obtained under normal cloudiness and Southern Ocean (STF RMBL) onshore flow conditions. Clear sky southerly refers to clear sky and Southern Ocean (STF RMBL) onshore flow conditions. Alk = 0.044 Mg^{++} , Sea SO₄ = 0.531 Mg^{++} , CaX = $\text{Ca}^{++} - 0.194 \text{ Mg}^{++}$, based on standard bulk seawater ion concentrations [Miller, 1974]. Soil SO₄ = 0.42 K^{+} and Ca⁺⁺Excess = $\text{CaX} - 1.67 \text{ K}^{+}$; see Table 2. Numbers in parentheses are $\pm 90\%$ confidence intervals. All concentrations are in nmol m^{-3} . BD is below detection limit of IC analysis; NSS(Mg) = $\text{SO}_4^- - \text{sea SO}_4 - \text{soil SO}_4$ (soil SO₄ was only $\sim 10\%$ (normal) and $\sim 5\%$ (clear sky)).

Baring Head sampling tower. This placed the impactor well above local sea spray influences for the “pumps-on” onshore wind direction [Allen *et al.*, 1997; J. Anderson, personal communication, June 2002]. Sampling over a 27-month period (2000–2002) allowed for a number of samples to be collected during clear-sky conditions in addition to an approximately equal number of samples during normal cloudiness conditions. Site meteorological data and AVHRR satellite data were considered for the field determination of clear-sky sampling periods. The impactor was manually and remotely started after an assessment was performed to declare initial clear-sky conditions. Satellite data analysis [Uddstrom *et al.*, 2001] was, subsequently, used to define percent cloud cover and declare clear-sky as well as normal cloudiness conditions. All clear-sky and normal cloudiness condition sampling was obtained with $>9 \text{ m s}^{-1}$ average wind speeds prevailing throughout ~ 15 -hour-long impactor sampling times. The 15-hour-long sampling time had been found [Sievering *et al.*, 1999] to provide sufficient aerosol mass on impactor filters to accurately estimate NSS values for $<0.4 \mu\text{m}$, 0.4 to $0.9 \mu\text{m}$, and 0.9 to $16 \mu\text{m}$ ambient diameter size fractions mentioned above under the very clean air conditions encountered over the Southern Ocean at Cape Grim (Tasmania). Whatman 41 filters were used throughout all sampling. Pumps-on conditions were set as the 135° – 280° (onshore flow) sector, with a 30-min delay to ensure clear-sky Southern Ocean sampling without continental aerosol contributions. Thus several days were required to obtain the 15-hour-long, in-sector impactor sampling.

2.3. Analysis

[8] Ion chromatography analysis was used for the determination of all anions and cations considered here. Sub-samples of the high-volume impactor filters were extracted in 5 mL of deionized water and inoculated with 50 μL of chloroform to prevent the bacterial degradation of methanesulfonic acid. Anions (chloride, bromide, nitrate and sulfate) were determined using a Dionex AS4A analytical column with an AG4A guard column and a 32 mM sodium

hydroxide eluent. Suppression with 20 mM sulfuric acid was used. Cations (sodium, ammonium, potassium, magnesium and calcium) were determined using a Dionex CS12 analytical column, protected with a CG12 guard column, using 20 mM methanesulfonic acid eluent and automatic suppression. Methanesulfonic acid was also assessed as a marker for biological sulfate. This was done using the Dionex AS4A column and an AG4A guard column with 5 mM sodium borate eluent and suppression with 40 mM sulfuric acid. In all cases the detector used was a Dionex conductivity detector.

[9] The determination of Baring Head NSS values used magnesium as the most conservative marker available for sea-salt sulfate. An assessment for the most appropriate marker was performed on previous aerosol samples collected at Baring Head (see Figure 3), as well as the samples collected for this work, using techniques detailed by Caine *et al.* [1999]. As at Cape Grim, the ratios of sodium, potassium, calcium, and chloride to magnesium were elevated above that in seawater. This effect was reduced for submicron sizes, further suggesting a soil influence, with chloride showing a typical ratio below that in seawater [Vogt *et al.*, 1996]. An additional factor precluding the use of sodium was the high blank associated with most glass fiber filters. Local soil samples from the cliff edge and from the narrow beach sand and soil “upwind” of the Baring Head sampling tower were collected to further assess the input of local soil to aerosol sampling.

[10] Blank subtraction was done using a substantially larger suite of blanks obtained at Cape Grim (during ACE-1) than could be obtained at Baring Head. The very same high-volume impactor instrumentation used at Baring Head had been previously used at Cape Grim to obtain this large number of blanks. The Cape Grim blank levels for the ions considered here (see Table 1) are based on the same 15-hour-long sampling time and essentially the same high wind speed conditions as were encountered at Baring Head [Sievering *et al.*, 1999]. Comparison of the few blanks obtained from Baring Head with those from Cape Grim showed that use of the larger suite of Cape Grim blanks was

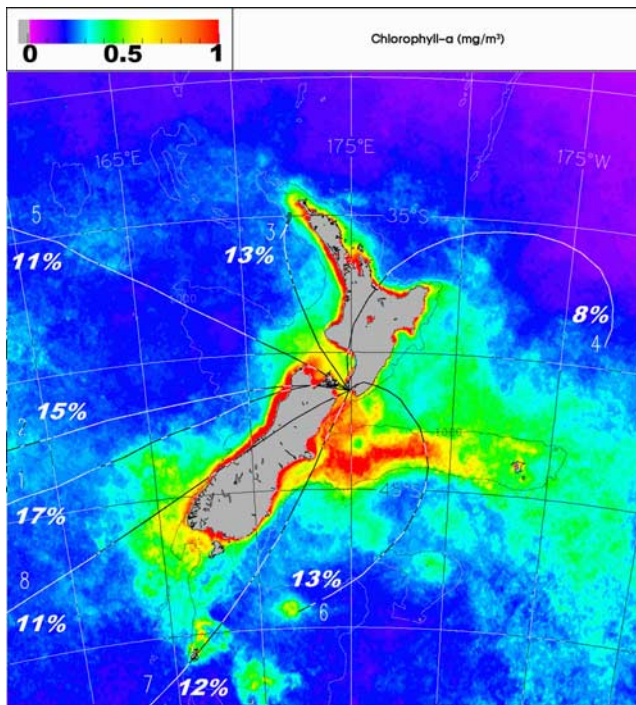


Figure 1. Ocean color composite of 1 year (2001) SeaWiFS Chlorophyll-a data overlain with the 1000-m bathymetry contour (thin black line) and with Baring Head, New Zealand, air mass trajectory climatology shown as the eight typical trajectory types determined by cluster analysis (see section 2.4 regarding this cluster analysis). Chatham Rise is that area within the 1000-m bathymetry “finger” contour line to the east of New Zealand’s South Island.

appropriate and presented less uncertainty into the ion concentration results (Table 1).

2.4. Meteorology

[11] Back trajectories with endpoint times of 00 Z and 12 Z were generated using analyzed wind fields calculated from primitive equations in a regional (Australia/New Zealand/Antarctica) numerical weather prediction model originally developed by the New Zealand Meteorological Service [Gordon, 1986]. The trajectories are 4-day back trajectories consisting of hourly values of position and pressure altitude and calculated for an endpoint altitude of 950 hPa. Considering a nominal MBL height of 1000 m (standard atmosphere pressure of 899 hPa), 97% of the hourly trajectory points, across all Baring Head back trajectories relevant to our sampling, were within the MBL for the 24-hour period prior to the end point time.

[12] Figure 1 includes (see eight curving lines with percent occurrence frequency numbers at their ends) an air mass back trajectory climatology for Baring Head using cluster analysis [Dorling *et al.*, 1992] of twice daily trajectories over a 10-year climatology. Of interest, are the cluster trajectories 6 and 7 that together brought clean marine air to the Baring Head site 25% of the 10-year period.

[13] The determination of percent clear-sky along back trajectories from the Baring Head site was estimated from

NOAA satellite data using a clear-sky detection algorithm developed by *Uddstrom et al.* [1999]. This algorithm uses AVHRR radiance and texture information in a Bayesian discriminant model to classify pixels as clear or cloudy. A small percentage of pixels are reported as missing due to failure of quality assurance tests or geometrical constraints on satellite coverage and data processing algorithms. The fraction of a 12 km by 12 km area, defined by a tile of 121 (11 × 11) pixels and centered at each hour along the back trajectories, having clear sky (number clear/total number clear plus cloudy) is then determined [Uddstrom *et al.*, 2001].

2.5. Primary Productivity of Ocean Surface Waters: Southern Ocean and the Subtropical Front Upwind of Baring Head

[14] The Southern Ocean surface waters’ annual primary productivity has been characterized for the major biogeochemical provinces [Moore and Abbott, 2000]. For open waters of the Southern Ocean (30–90° S) the mean annual primary productivity is given by Moore and Abbott [2000] as 131 gC m⁻² yr⁻¹. This is the same as primary productivity estimates for the global oceans’ open waters with an annual primary productivity of ~130 gC m⁻² yr⁻¹ [e.g., Schlesinger, 1997]. However, the surface waters along back trajectories from Baring Head and for onshore flow conditions, constitute a region of substantially greater annual primary productivity. It is well known that a highly productive and quite stationary ocean subtropical front is constrained by the bathymetry of the Chatham Rise (see the 1000-m bathymetry contour in Figure 1). As a result, SEAWIFS satellite chlorophyll-a (Chl) concentrations are enhanced in the surface waters upwind of Baring Head (see the color coded Chl concentrations, mg m⁻³; especially the yellow, orange, and red colored areas within the 1000-m bathymetry contour of the Chatham Rise). These Chl concentration data may be used to calculate annual primary productivity values. The procedure is referred to as the vertically generalized production model (VGPM) and is detailed by *Behrenfeld and Falkowski* [1997]. Inputs to the VGPM are satellite-based, surface water Chl concentrations, sea surface temperatures, and photosynthetically active radiation. Using the VGPM with the 2001 Chl data of Figure 1, one arrives at an annual primary productivity for the region upwind of Baring Head falling in the 350–400 gC m⁻² yr⁻¹ range. Direct primary productivity measurements are limited. For the subtropical front, *Bradford-Grieve et al.* [1997] provide some of the best data, although even their data are limited to two stations on the subtropical front. From these spring and winter measurements, the annual primary productivity of the subtropical front is estimated to be less than 350 gC m⁻² yr⁻¹ with variability across the seasons. Yet the subtropical front behaves much like the midlatitude coastal waters, which Moore and Abbott [2000] indicate have an annual primary productivity of 505 gC m⁻² yr⁻¹. Thus an annual primary productivity value for the subtropical front of 350–400 gC m⁻² yr⁻¹ is deemed a good annual estimator.

[15] In summary, the surface waters upwind of the Baring Head sampling location have an annual primary productivity that is approximately three times that for the

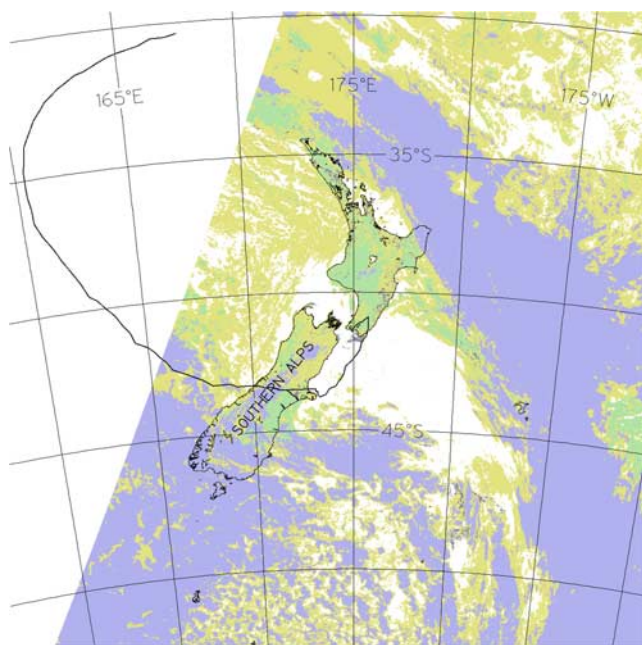


Figure 2. Case study of “clear sky southerly” sample at Baring Head (15 Mar 2001) with NOAA satellite image analyzed by SRTex: white is 100% clear sky; periwinkle is <10% clear sky; gray is missing data. The back trajectory at the time of this image is in the clear-sky patch to the east of the South Island 22 hours before arrival at Baring Head. Meteorological conditions for this 15 March 2001 sample were approximately at the mean values for the entire sampling campaign ($U = 10.9 \text{ m s}^{-1}$, $RH = 80.2\%$ and $T = 14^\circ\text{C}$).

open waters of the global oceans (i.e., a ratio of $350\text{--}400 \text{ gC m}^{-2} \text{ yr}^{-1}$ over $130 \text{ gC m}^{-2} \text{ yr}^{-1}$ or approx. 3). This 3-fold greater surface ocean primary productivity provides the RMBL region upwind of Baring Head with substantially more S emissions [Harvey *et al.*, 2002] and, it shall be shown in section 3.3, may also provide substantially more biogenically derived alkalinity than for typical open ocean RMBL conditions. This will be a consideration in the extrapolation of Baring Head results to other regions of the RMBL (see section 3.5).

2.6. Statistical Analysis and Typical RMBL Sea-Salt Aerosol Data

[16] Standard statistical procedures with Statgraphics 5.0 software (Manugistics Inc.), including one-tailed p value regression diagnostics, were used throughout all analysis and interpretation of the Baring Head data. These procedures were particularly helpful in the statistical analysis of the Asian Aerosol Characterization Experiment (ACE-Asia) data obtained aboard the NOAA ship RV *Ronald H. Brown* in the RMBL of the North Pacific Ocean during its transit from Hawaii to Japan, March–April of 2001 [Quinn *et al.*, 2004]. A Berner cascade impactor (30 lpm flow rate), with 50% aerodynamic diameter size cuts (at 80% average ambient relative humidity) of 0.22, 0.37, 0.66, 1.4, 3.0, 6.2, and $15 \mu\text{m}$ and with Tedlar films used as collection filters, sampled air on either a 12-hour or a

24-hour time base [Quinn *et al.*, 2004]. Sodium was here used as the marker for sea-salt sulfate. Statistical analysis was performed using the aggregate $1.4\text{--}15 \mu\text{m}$ diameter ion data, considered to be approximately the aerosol size range of the coarse sea-salt aerosol sampled by the high-volume impactor and, also, a size range that was not affected by accumulation mode NSS.

3. Results and Discussion

3.1. Meteorological Setting

[17] Over the entire period of sampling (27 months), wind speeds were often $>9 \text{ m s}^{-1}$. The overall mean wind speed (U) was $\sim 11 \text{ m s}^{-1}$ during actual high-volume impactor aerosol sampling times. These wind speeds also prevailed over the Southern Ocean upwind of Baring Head. The mean dry deposition velocity of sea-salt aerosols was about 2 cm s^{-1} ; the mean MBL lifetime was thus just under 20 hours (estimated range of 10 to 28 hours across all samples). There were many periods during which the 4-day-long back trajectories indicated over water fetches upwind of Baring Head had prevailed for more than 20 hours. Again, cluster back trajectories 6 and 7 of Figure 1 provide this over ocean fetch at Baring Head with the previously mentioned occurrence frequency of 25%. However, this includes periods with $U < 9 \text{ m s}^{-1}$. A number of individual trajectories within these two clusters pass over the Southern Alps. This alpine mountain chain, down the length of the South Island (Figure 2), extends to heights above 2000 m and has a major influence on regional meteorology, including wind flow and rainfall [Wratt *et al.*, 1996]. During prevailing westerly flow, there is a major orographic enhancement of rainfall on the west coast and dry foehn winds to the east. The ideal situation of dry atmospheric conditions to the east of the Alps causing clear-sky conditions along with high wind speed transport over water toward Baring Head occurred occasionally (see the example in Figure 2). In general, actual trajectories did have the anticyclonic curvature of cluster trajectories 6 and 7, with descending air and an origin in the free troposphere. This trajectory often meant less cloudy skies.

[18] From local observation and remote sensing of clouds at the time of sampling, a group of sampling periods was designated as clear sky southerly. For these periods, the clear-sky detection algorithm [Uddstrom *et al.*, 2001] successfully processed satellite imagery data whenever “satellite of opportunity” overpasses provided such data. However, a large majority of the back trajectory hourly cloud fraction analysis area ($12 \text{ km} \times 12 \text{ km}$) had no accompanying satellite imagery data. Thus it was decided to aggregate all cloud fraction results relevant to each high-volume impactor sampling period. Given that back trajectories were provided at 00 Z and 12 Z of each day within the several days long, high-volume impactor exposure periods, a large number of cloud fraction values were available for the actual high-volume sampling time intervals. A mean back trajectory duration of 24 hours was considered here given the quite rapid heterogeneous reaction times and the short <20 hour mean lifetime of sampled sea-salt aerosols, and the fact that the back trajectories were within the MBL 97% of the 24-hour duration time.

[19] Across the whole of the high-volume impactor sampling intervals, the aggregate mean clear-sky fraction (based

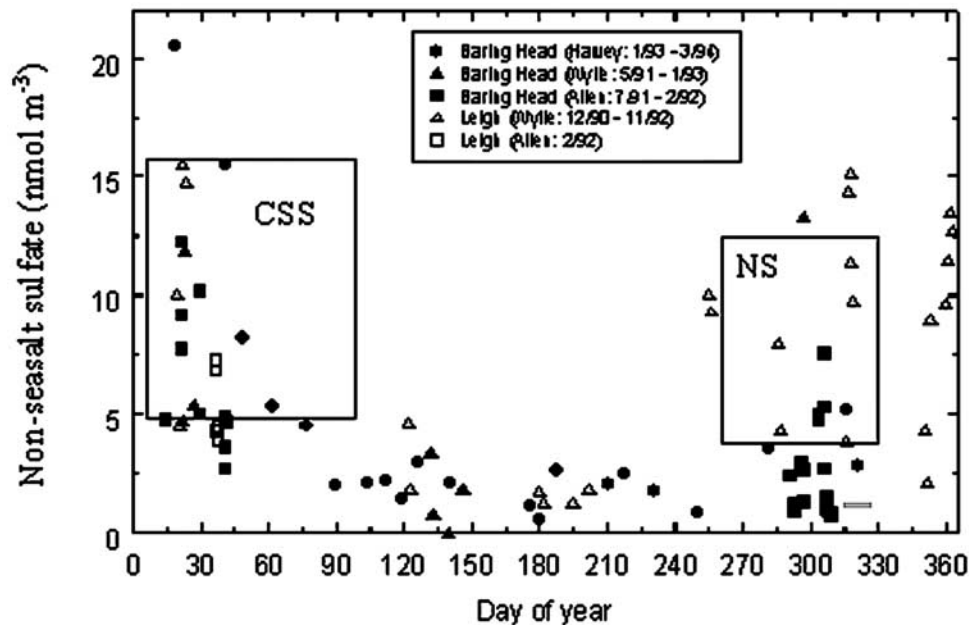


Figure 3. Total (<0.1–16 μm diameter) NSS in sea-salt aerosols found in five previous studies at the Baring Head and Leigh, New Zealand coastal sites with open ocean fetch (data points) and the total NSS found in this study; see the two rectangular boxes where CSS is clear sky southerly and NS is normal southerly. These boxes show the range in both NSS concentrations and sampling day of year observed across this 27-month Baring Head study (NSS mean and 90% confidence interval values are found in Table 1).

on a single pixel available for each trajectory coordinate) was 0.14 ± 0.18 . This 14% figure is within the <15% clear-sky figure for a typical year in the Southern Ocean RMBL area upwind of Baring Head (see “STW [east]” ocean area results of *Uddstrom et al.* [2001]).

[20] No processing of satellite imagery data was done to identify cloud fractions for the “normal cloudiness” high-volume impactor sampling periods with southerly airflow (hereafter, designated as normal southerly). Many days of overall exposure time were included in the normal cloudiness total sampling times, and we assume the cloud fraction during most of the normal cloudiness sampling periods was also within the <15% figure [*Uddstrom et al.*, 2001].

[21] Despite this satellite clear-sky analysis outcome, support for the distinction between clear sky southerly and normal southerly was obtained from analysis of the local daytime measurement of solar radiation at Baring Head. For this analysis, clear-sky conditions were defined as solar radiation flux within 70% of the theoretical maximum flux at the ground. For the clear sky southerly samples, the average clear-sky duration was $70 \pm 32\%$ of daytime, whereas, for normal southerly samples, this value was $26 \pm 21\%$. In spite of the high cloud occurrence frequency in the region, there was significantly greater exposure to a window of clear sky for clear sky southerly by a factor of about two and a half (i.e., 70%/26%), based on this local measurement. Analysis of satellite images confirms that a majority of the samples designated clear sky southerly did encounter a significant expanse of clear sky in the 24 hours prior to sampling. This is shown in

Figure 2 for the clear sky southerly sample of 15 March 2001.

3.2. Contributions to Observed Coarse-Aerosol NSS

[22] Table 1 presents the average ion concentrations, in nmol m^{-3} , for the normal southerly and clear sky southerly samples obtained throughout the 27-month sampling period. The four coarse aerosol impactor stages were aggregated to provide the 0.9–16 μm diameter results shown. The mean wind speed during normal southerly sampling was 11.3 m s^{-1} , whereas during clear sky southerly sampling, it was 10.8 m s^{-1} .

[23] The long-term mean NSS found at Baring Head under southerly flow conditions is 7.3 nmol m^{-3} [*Gomez*, 1996] (Figure 3). In comparison, the Table 1 normal southerly mean NSS is 3.8 nmol m^{-3} , about half of the long-term average. However, the clear sky southerly mean NSS is 11.7 nmol m^{-3} , about 3 times the normal southerly mean NSS. The clear sky southerly NSS concentrations for all three size fractions shown in Table 1 are markedly different (at 90% conf.) and higher than those for normal southerly conditions. Finally, the portion of NSS found in coarse (0.9–16 μm ambient diameter) aerosols is noteworthy. These 2.6 and $8.4 \text{ nmol NSS m}^{-3}$ concentrations for normal southerly and clear sky southerly conditions, respectively, are large magnitudes, considering that clean Southern Ocean air was the source region [*Sievering et al.*, 1999]. Some of this normal/clear sky difference may be caused by seasonality in the DMS source. The clear-sky samples were collected during austral summer and fall, whereas the normal southerly samples were collected during austral spring.

[24] Three previous high-volume impactor data sets under clean air (onshore) Southern Ocean flow conditions have been published for New Zealand coastal sampling sites: the data of *Allen et al.* [1997] at Baring Head, *Wylie and de Mora* [1996] at Baring Head, and Harvey at Baring Head [Gomez, 1996]. These data sets all indicate that quite large coarse aerosol NSS concentrations prevail at Baring Head, at least during the spring and summer. In addition, more than $\frac{1}{4}$ of the total summertime NSS at Baring Head had been previously found in >3.5 μm diameter aerosols by *Allen et al.* [1997]. Harvey observed that about 15% of total summertime NSS at Baring Head was found in the 7–16 μm diameter range, with 80% in >0.5 μm aerosols.

[25] The data points of Figure 3 show the three published Baring Head high-volume impactor NSS data sets along with the unpublished onshore flow, high-volume impactor data of Wylie obtained at Leigh, NZ (on the northeast coast of the North Island - with ocean fetch to the northeast, see cluster 4 in Figure 1, which also has anticyclonic flow) and by Allen at Leigh. The Figure 3 data points show, during austral spring (Julian days 243–334) and summer (J 335–59), that total NSS concentrations of as much as 15 nmol m^{-3} (on rare occasions, even higher) have been observed. Figure 3 also shows the range in NSS values found in this study; see the rectangular boxes labeled with CSS (clear sky southerly) and NS (normal southerly). These boxes display the full range in both NSS concentrations found and sampling day of year across this 27-month study (numerically presented in Table 1). A scan of the Figure 3 data clearly shows that quite large variability in total NSS is to be expected during spring and summer. Mechanism(s) that may explain these high NSS concentrations, the high percentage of total NSS found in coarse aerosols, and, also, the large variability in total NSS found at New Zealand coastal sites under onshore flow conditions are all in need of discussion.

[26] The portion of coarse NSS found in the MBL that may be attributed to O₃ oxidation in sea-salt aerosol water during the sea-salt aerosol's lifetime has been argued to be about 20% beyond its bulk seawater-derived alkalinity [Chameides and Stelson, 1992], where this alkalinity is, again, given by $0.005 [\text{Na}]$ or (equivalently) by $0.044 [\text{Mg}]$ [Millero, 1974]. This additional $\sim 20\%$ NSS by O₃ oxidation in sea-salt aerosol water is due to thermodynamic equilibrium between gaseous CO₂ and aqueous CO₂ and the resulting shift in the $[\text{HCO}_3^-]/[\text{CO}_3^{2-}]$ ratio as the sea-salt aerosol evolves and water evaporates [Sievering et al., 1999]. Given the bulk seawater alkalinity (Alk) values in Table 1, it would appear that only $\sim 7\%$ of the normal southerly coarse NSS and only $\sim 2\%$ of the clear sky southerly coarse NSS may be attributed to the O₃ oxidation pathway, unless additional sources of alkalinity were present in the sea-salt aerosol water of these samples. Further, only $\sim 1\%$ of the fine NSS and much less than 1% of the very fine NSS (for both normal southerly and clear sky southerly conditions) may be attributed to O₃ oxidation in sea-salt aerosol water, again, unless additional alkalinity was present in sea-salt aerosol water.

[27] The contribution of cloud production/processing to the NSS found in all three aerosol size fractions of clear sky southerly samples would have been quite small. Regarding the coarse aerosol NSS, a number of studies [e.g., Hoppel et

al., 1994] do not show any supermicron aerosols resulting from cloud production/processing. *Gurciullo et al.* [1999], for Southern Ocean conditions quite similar to those encountered at Baring Head, showed that either ammonia (NH₃) in the ambient air or alkalinity in sea-salt aerosols is required to allow SO₂ oxidation to proceed in cloud droplets. The concentration of NH₃ in the Southern Ocean MBL is very low; *Ayers and Gras* [1983] found [NH₃] in “baseline” air at Cape Grim is only about 60 ng m^{-3} , with no seasonal trend. *Allen et al.* [1997] obtained 40 ng m^{-3} for clean southerly samples collected at Baring Head. This small amount of ammonia would be consumed in producing the fine and very fine aerosol NSS observed in normal southerly samples. Further, whatever the alkalinity that may be found in sea-salt aerosol water, it should be consumed within the first tens of minutes [Chameides and Stelson, 1992] after emission from the sea surface by the O₃ oxidation mechanism and long before it reaches cloud base. *Sievering et al.* [1999] concluded that, on average, only about 0.1 nmol m^{-3} of the Southern Ocean MBL's coarse aerosol NSS could be derived from cloud production/processing. Applied to Baring Head, this suggests that 5%, or less, of the normal southerly coarse aerosol NSS and about 1% of the clear sky southerly coarse aerosol NSS may be attributed to cloud production/processing. Another possibility, scavenging of gaseous H₂SO₄, was, almost surely, not a significant contributor to coarse aerosol NSS since the average [H₂SO₄] in the Southern Ocean MBL is <0.1 pptv (F. Eisele, personal communication, November 2001).

3.3. Role of Alkalinity From Ocean Surface Water Primary Productivity

[28] A substantial portion of the NSS is still unexplained. O₃ oxidation in sea-salt aerosol water (considering bulk seawater alkalinity) and cloud production/processing, together, can explain only 10–15% of the observed normal southerly coarse aerosol NSS and $<4\%$ of the observed clear-sky coarse aerosol NSS. Further, only a minor portion of the fine and, perhaps also, of the very fine NSS observed during clear sky southerly sampling may be explained by these processes.

[29] The Ca⁺⁺ and Mg⁺⁺ data in Table 1 suggest a possible explanation. The molar ratio of coarse aerosol Ca⁺⁺ to Mg⁺⁺ is ~ 2 and ~ 7 for normal southerly and clear sky southerly samples, respectively, versus the bulk seawater molar ratio of ~ 0.2 . If the portion of Ca⁺⁺ (noting that “Ca⁺⁺” implies soluble Ca versus “Ca” which includes insoluble calcium) observed at Baring Head that is sea derived is greater than that derived from bulk seawater, then additional alkalinity is available for NSS production by O₃ oxidation in sea-salt aerosol water. To determine this total sea-derived Ca⁺⁺, the contributions to Ca⁺⁺ from bulk seawater and from local soil must be specified. Bulk seawater-derived Ca⁺⁺ was determined using the seawater ionic ratios given by *Millero* [1974]. The CaX column in Table 1 is this excess Ca⁺⁺, in nmol m^{-3} , once correcting for bulk seawater Ca⁺⁺. This CaX is about 90% and $>95\%$ of total Ca⁺⁺ in all three size fractions for normal southerly and clear sky southerly samples, respectively.

[30] Local soil cation and anion concentrations were determined by ion chromatography analysis of five soil samples from the cliff edge and from the narrow beach sand

Table 2. Baring Head Local Soil Ion Concentrations and Molar Ratios Relative to K⁺^a

Ion	Concentration, μg (g soil) ⁻¹	Molar Ratio, mol mol ⁻¹
Na ⁺	54.1 (±11.9)	5.60 (±2.0)
Ca ⁺⁺	27.3 (±8.1)	1.67 (±0.68)
Mg ⁺⁺	9.5 (±3.8)	0.91 (±0.42)
K ⁺	16.4 (±4.5)	1.00 (±0.28)
SO ₄ ⁻	19.0 (±4.8)	0.42 (±.16)
NH ₄ ⁺	1.7 (±1.3)	0.23 (±.19)

^aNumbers in parentheses in the second column are ±90% confidence intervals, and in the third column they are RMS uncertainties.

and soil “upwind” (i.e., immediately to the south) of the Baring Head sampling tower. The second column in Table 2 shows the μg (g soil)⁻¹ and the 90% confidence interval values for the ions of importance to this study. Note that the K⁺ concentration is relatively low in bulk seawater (its mass ratio to Mg⁺⁺ in bulk seawater is 0.31 so that only a small fraction of the 16.4 μg K⁺ (g soil)⁻¹ found in local soil could be derived from bulk seawater.) Thus K⁺ is designated as the Baring Head soil marker. The third column of Table 2 shows molar ratios of the other ions to that of K⁺ with RMS uncertainty shown in parentheses. Reasonable estimates of local soil-derived Ca⁺⁺ and SO₄⁻ contributions to Baring Head aerosol sampling were possible given that K⁺ concentrations for normal southerly and clear sky southerly samples are available (Table 1). Using these K⁺ values and the BD (below detection of IC) values, one may determine the Ca⁺⁺ in excess of both bulk seawater and local soil; i.e., sea-derived Ca⁺⁺ excesses (Ca⁺⁺Excess). These Ca⁺⁺Excess values are shown in Table 1.

[31] The local soil SO₄⁻ source contributed 21% of the coarse SO₄⁻ observed during normal southerly sampling but only 11% of the coarse SO₄⁻ observed during clear sky southerly sampling. Local soil plus bulk seawater was the source of a substantial part of the observed normal southerly Ca⁺⁺ at Baring Head but they contributed in only a minor way to clear sky southerly Ca⁺⁺. Just over 40% of the normal southerly and 80–85% of the clear sky southerly Ca⁺⁺ remains unexplained. This large remainder Ca⁺⁺ can only have been sea derived.

[32] Calcium carbonate (CaCO₃) is produced as scales by coccolithophore phytoplankton including the abundant *Emiliania huxleyi*. These CaCO₃ structures build up on the exterior of coccolithophores by exudation from within the cells. The scales grow, typically, to 0.3–0.5 μm across, sometimes larger. They are quite delicate and can continually slough off the organism. In addition to sloughing, various processes can release scales into the water. The plankton can be subjected to viral attack which gives rise to cell lysis. This can literally cause the plankton cells to blow apart, spilling their contents and surface scales into the ocean’s surface waters. The plankton may also be subject to grazing by microzooplankton, with breakup resulting in the release of scales. There is *in situ* evidence of the abundance of coccolithophores around the Subtropical Front [Findlay and Giraudeau, 2000]. Chang *et al.* [2003] have also found coccolithophores on the shelf waters around New Zealand. More broadly, Brown and Yoder [1994] have observed their abundance by remote sensing of ocean colors resulting from coccolithophores.

[33] It has been known for some time [MacIntyre, 1974] that this “calcareous plankton debris” (including scales) accumulates in the sea’s surface microlayer. Further, Ca⁺⁺ binds strongly to organic molecules that also concentrate in the surface microlayer [e.g., MacIntyre, 1974]. The initial jet drop as well as most subsequent film drops produced by bursting bubbles are endowed with this surface microlayer material [Warneck, 1988]. Jet drops have a broad size distribution with a maximum at 3–5 μm diameter; film drops also have a broad size distribution but with a maximum in the 0.2–1 μm diameter range, depending on relative humidity [O’Dowd *et al.*, 1997]. It may thus be expected that Ca⁺⁺ Excess, and alkalinity, will be enriched in Baring Head coarse, very fine and, perhaps less so, in the fine sea-salt aerosols. Others have reported a nonsoil Ca⁺⁺ excess in aerosols over the Atlantic and Pacific Oceans [e.g., Junge, 1972; Duce and Hoffman, 1976; Maenhaut *et al.*, 1983].

[34] The magnitude of sea-derived Ca⁺⁺ excess over that from bulk seawater in coarse aerosols at Baring Head is a factor of about 4.5 and 30 for normal southerly and clear sky southerly samples, respectively (i.e., Ca⁺⁺Excess/[Ca⁺⁺ – CaX] determined from values in Table 1). The discrepancy in enrichment factor under clear sky versus normal southerly conditions is, in part, caused by cloud and precipitation scavenging of soluble Ca⁺⁺. Another factor may be differences in surface waters’ primary productivity upwind of Baring Head during the, mainly, springtime normal southerly sampling and the, mainly, summertime clear sky southerly sampling. Indeed, the large variability in Ca⁺⁺Excess values is derived, in large measure, from variability in the Ca⁺⁺ data. This variability was very likely introduced by the changing primary productivity of surface waters upwind of Baring Head. Aircraft measurements (which may integrate primary productivity impacts on aerosol chemistry) over the broader Southern Ocean [Cattell *et al.*, 1977] indicated a Ca⁺⁺ enrichment factor of 2.4 (±0.5) for coarse aerosols.

[35] The Ca⁺⁺Excess in fine and very fine aerosols could not be quantified for normal southerly Baring Head samples. For clear sky southerly, sufficient Ca⁺⁺Excess was present in fine and very fine aerosols such that O₃ oxidation could account for essentially all of the NSS observed in these size fractions. The Ca⁺⁺Excess/(Ca⁺⁺ – CaX) ratios (see Table 1) of roughly 25–30 for fine aerosols and 40–45 for very fine aerosols in clear sky southerly samples suggest a possible trend of increasing Ca⁺⁺ enrichment with decreasing aerosol size. (Such a trend is clearly counter to that from soil-derived Ca.) Maenhaut *et al.* [1983] found this trend by size in a suite of Pacific Ocean RMBL aerosol samples without soil input. Such an aerosol size dependent Ca⁺⁺Excess trend may possibly be explained by sea-salt aerosol production processes at the air-sea interface. Henricks and Williams [1985] observed that small plankton CaCO₃ fragments (plankton debris) are more soluble than larger fragments in surface microlayer seawater. Further, small seawater bubbles have been found to be effective in transporting sea surface microlayer material into the air [Tseng *et al.*, 1992].

[36] The enrichment of Ca⁺⁺ for all size fractions of clear sky southerly aerosol samples appears to have provided sea-salt aerosol water with sufficient additional alkalinity to

allow continued rapid O₃ oxidation of sulfur gases to NSS in that sea-salt aerosol water. The pH of sea-salt aerosol water then remains at about 8 [Chameides and Stelson, 1992]. The contribution of NSS production by the O₃ oxidation pathway is essentially complete within 10–15 min. At this point the pH of sea-salt aerosol water drops and O₃ oxidation is quenched. Production of NSS in sea-salt aerosol water at Baring Head during clear sky southerly conditions may have been limited by the availability of gaseous sulfur since only 16.8 neq NSS m⁻³ was produced in the presence of the approx. 60 neq alkalinity m⁻³ (the mean gaseous S found by DeBruyn *et al.* [2002] at Baring Head was about 14 neq m⁻³). It is important to note, again, that O₃ oxidation occurs rapidly in the sea-salt aerosol water associated with sea-salt aerosols. The sea-derived Ca⁺⁺Excess can supply alkalinity to NSS production by cloud processing only after near surface and in sea-salt aerosol water production has consumed all available sulfur. Under normal cloudiness conditions, when coarse aerosols reach cloud base, essentially all of the Ca⁺⁺Excess due to calcareous plankton debris may already have reacted. Thus cloud processing of sea derived Ca⁺⁺Excess may, generally, not be a factor under typical RMBL conditions.

[37] Artaxo *et al.* [1992] performed individual particle analysis as well as elemental analysis on a large number of aerosol samples from the RMBL of the Weddell Sea and Southern Ocean. Source apportionment of >2 μm dry diameter (at 80% RH, >~4.5 μm ambient diameter) aerosol mass concentration using elemental data showed that 85–90% and ~5%, respectively, of this mass was accounted for by sea-salt and soil dust aerosols. For the <~4.5 μm diameter aerosols, sea-salt accounted for 60%, sulfates 25–30%, and soil dust only ~1%. Further, electron probe X-ray microanalysis of these <~4.5 μm diameter aerosols showed a variety of sulfate aerosol types with CaSO₄, CaSO₄ + NaCl, and CaSO₄ + MgCl₂ among nine cluster analysis determined aerosol groups. In fact, most of the sulfur in >0.15 μm aerosols was in the form of CaSO₄.

3.4. Contribution of O₃ Oxidation in Sea-Salt Aerosol Water to Observed NSS at Baring Head

[38] The NSS results of Table 1 may now be considered in the context of the section 3.3 discussion (and also considering uncertainty in results). To do so requires that the term “bulk seawater” alkalinity is now referred to as “seawater nonbiogenic alkalinity” and that results will be presented in neq m⁻³ as well as nmol m⁻³.

[39] For normal southerly conditions, the total coarse aerosol alkalinity was 6.32 ± 6.17 nmol m⁻³ or 12.32 neq m⁻³ (i.e., seawater nonbiogenic alkalinity of 0.32 ± 0.13 neq m⁻³ plus the biogenically derived Ca⁺⁺Excess of 12.0 ± 12 neq m⁻³). This is sufficient to allow O₃ oxidation in sea-salt aerosol water to have produced the observed coarse aerosol 5.2 ± 2.2 neq NSS m⁻³. The total fine aerosol alkalinity was about 0.08 neq m⁻³. It is possible that O₃ oxidation in sea-salt aerosol water may have contributed about 10% of the fine aerosol 0.8 ± 0.4 nmol NSS m⁻³. The contribution of O₃ oxidation to the very fine aerosol NSS of 1.6 ± 0.6 nmol m⁻³ may have been of order 10%. Uncertainty in the magnitude of alkalinity present makes these latter conclusions only qualitative.

[40] For clear sky southerly conditions, the total coarse aerosol alkalinity was just over 30 nmol m⁻³ or about 60 ± 37 neq m⁻³. This is more than sufficient to allow O₃ oxidation in sea-salt aerosol water to have produced all observed coarse aerosol NSS of 16.8 ± 6.2 neq m⁻³. The total fine aerosol alkalinity was, roughly, 5 neq m⁻³. Thus O₃ oxidation in sea-salt aerosol water may have produced all of the fine aerosol 2.2 ± 0.8 neq NSS m⁻³. The total very fine aerosol alkalinity was probably of order 4 neq m⁻³. It is again possible that all of the very fine aerosol 4.4 ± 1.8 neq NSS m⁻³ may have been produced by O₃ oxidation in sea-salt aerosol water. However, only the coarse aerosol result may be considered significant.

[41] In summary, essentially all coarse aerosol NSS found under clear sky southerly conditions may be attributed to O₃ oxidation in sea-salt aerosol water. This conclusion is noteworthy in that over 8 nmol NSS m⁻³ is estimated to have been produced by O₃ oxidation in sea-salt aerosol water.

3.5. Extrapolation to Typical RMBL Sea-Salt Conditions

[42] It is quite unique to have had such high wind speeds (11 m/s) and clear-sky conditions for the air encountered by sea-salt aerosols along their back trajectories from Baring Head over the Southern Ocean. The clear sky southerly data of Table 1 show that a very substantial sea-derived Ca⁺⁺Excess, of order 30 nmol m⁻³, may accumulate in the sea-salt aerosol water of coarse sea-salt aerosols when precipitation and cloud processing have only a minimal influence and there is substantial surface waters’ primary productivity upwind of an MBL sampling site. This clear sky Ca⁺⁺Excess allowed O₃ oxidation in sea-salt aerosol water to continue to produce NSS, limited only by the available gaseous sulfur. Very large amounts (for the RMBL) of coarse aerosol NSS may then be produced by O₃ oxidation. This consumption of large amounts of gaseous sulfur may have implications for new particle formation. The generation of aerosol NSS in clear sky southerly conditions is limited by the immediate availability of sulfur dioxide. Once this sulfur dioxide is incorporated into sea-salt aerosols, there is, then, effectively none available for new particle formation by nucleation.

[43] It is desirable to consider measurements under typical RMBL conditions and with typical sea-salt ion content representative of open ocean conditions. Size-distributed aerosol samples meeting this criterion were obtained during the Western North Pacific transit cruise of the NOAA ship *Ronald Brown* from Hawaii to Japan (from ~170°W to ~145°E along 33–34°N) for participation in the ACE-Asia experiment [Quinn *et al.*, 2004]. Fifteen Berner impactor [Berner *et al.*, 1979] samples were collected over periods of 12-hours (mainly) or 24-hours during Julian days 79 to 91 of 2001. Individual particle analysis of transit cruise coarse aerosol samples (J. Anderson, personal communication, September 2002) had shown that two samples had very large Asian dust inputs (e.g., the total Al values for these two samples were >5σ and ~4σ outliers, respectively, above the mean Al for all transit samples) and were discarded from this analysis. Coarse aerosol data were obtained by aggregating ion concentrations found on the top four stages of the Berner impactor, resulting in coarse aerosol collection with

Table 3. Berner Impactor Coarse Aerosol Ion Data by Ion Chromatography Analysis for Coarse NSS, Alk, and CaX With Coarse (Insoluble Plus Soluble) Ca and Total Al Data by XRF Analysis for the Hawaii to Japan ACE-Asia Cruise of 2001^a

Sample	Coarse NSS	Coarse Alk	Coarse CaX	XRF Coarse Ca	Total Al
3	0.31	0.65	0.01	2.77	2.00
4	0.66	0.61	0.35	3.02	2.50
5	1.10	0.78	0.73	4.46	4.63
6	0.92	0.52	1.01	3.52	4.30
7	2.74	0.80	2.32	12.3	24.0
9	3.87	0.80	1.73	7.38	11.5
10	1.96	0.50	1.34	4.26	7.18
11	1.70	0.58	1.54	4.16	4.28
12	2.12	0.86	1.54	5.51	5.30
14	2.79	0.57	2.04	7.08	8.00
15	1.79	0.18	1.57	2.22	3.56
16	1.73	0.26	2.34	5.61	12.7
17	3.59	0.15	2.96	7.85	17.4

^aAll concentrations are in nmol m⁻³. CaX = Ca⁺⁺ - 0.194 Mg⁺⁺.

ambient cut points at ~1.4 μm diameter and at ~15 μm diameter. The data for Coarse NSS, seawater-derived non-biogenic alkalinity (Coarse Alk), Coarse CaX, and for XRF-determined coarse Ca (XRF Coarse Ca) and Total Al (soil marker element) are shown in Table 3.

[44] The mean coarse aerosol CaX was 1.49 nmol m⁻³; for XRF Coarse Ca it was 5.39 nmol m⁻³. The mean coarse aerosol NSS (using Na⁺ as the sea marker), total Al, and Coarse Alk were 1.94, 8.06 and 0.56 nmol m⁻³, respectively. On the basis of a Ca to Al molar ratio of about 1 to 2 for Asian dust [Xuan and Sokolik, 2002; I. Sokolik, personal communication, November 2002], about three fourths of the XRF Coarse Ca may have been contributed by Asian dust. However, CaX (i.e., Ca⁺⁺ - 0.194 Mg⁺⁺), soluble Ca determined by ion chromatography analysis, was only about one fourth of the XRF Coarse Ca, suggesting that Asian dust was probably, in large part, insoluble.

[45] Multiple regression analysis, using both forward and backward stepwise procedures for variable selection [Kleinbaum et al., 1998], returned the following model of coarse aerosol NSS dependence:

$$\text{Coarse NSS} = -0.69 + 1.23(\text{CaX}) + 1.41(\text{Alk}) \quad p = 0.0009 \quad (1)$$

The probability that either multiple regression variable does not belong in this model is small (p[CaX] = 0.0002, p[Alk] = 0.049). The multiple R² is 0.78 with the constant insignificant (p = 0.17). Lack of fit testing showed there is no need to consider a nonlinear term in either CaX or Alk.

[46] Equation (1) indicates the NSS produced by Ca⁺⁺ excess is 1.83 ± 0.34 nmol m⁻³ (95% conf.), while that produced by bulk seawater alkalinity is 0.79 ± 0.43 nmol m⁻³ (95% conf.). Thus the 100% to 250% additional alkalinity provided by CaX enhanced the NSS found in coarse aerosols by a factor of 2.3 ± 1.7 or about 1.5–2 nmol m⁻³. The forced addition of Al as a surrogate for soil alkalinity as a third possible explanatory variable showed it to be quite insignificant (p = 0.39), with a negative coefficient (a negative (contradictory) coefficient also appears when XRF Coarse Ca is considered as a forced variable). Further, the correlation of Coarse CaX with XRF

Coarse Ca is poor (r² = 0.44). It appears that Asian dust was an insignificant alkalinity contributor to sea-salt aerosol water and the maintenance of NSS production by O₃ oxidation. This indicates that the Asian dust Ca encountered was largely, if not wholly, insoluble in seawater. It must have provided far less alkalinity to sea-salt aerosol water than did calcareous plankton debris.

[47] In contrast, fragmented calcareous plankton debris (especially the very small fragments found in the surface microlayer) is quite soluble [Henricks and Williams, 1985]. Indeed, the 1.23 ± 0.21 (95% confidence) regression coefficient for CaX indicates the fragmented plankton debris was, effectively, 100% soluble in sea-salt aerosol water. That is, the CaX found in coarse aerosols should provide alkalinity such that the NSS produced by O₃ oxidation is, on a molar basis, equal to that soluble CaX from calcareous plankton debris, yielding a regression coefficient near to 1.0. The 1.23 ± 0.21 coefficient in equation (1) suggests an NSS yield that may even be somewhat greater than the level of alkalinity provided by fragmented plankton debris.

[48] These regression results using western North Pacific RMBL coarse aerosol impactor data indicate that about 1.5–2 nmol m⁻³ additional NSS may be found in coarse aerosols of the RMBL due to enhanced O₃ oxidation in sea-salt aerosol water. Sea-derived CaX (beyond seawater-derived, nonbiogenic alkalinity) is indicated to be responsible for the excess alkalinity which allows O₃ oxidation in sea-salt aerosol water to produce substantially more NSS than if only seawater nonbiogenic alkalinity was present. These results for more typical RMBL conditions are supported by modeling analyses [von Glasow and Crutzen, 2004] using the MISTRA-MPIC model [von Glasow et al., 2002] with the remote MBL meteorological (including typical cloudiness) conditions and chemical setting of Cape Grim. The addition of 100 and 150% biogenic alkalinity beyond seawater nonbiogenic alkalinity increased the model's relative contribution to total sulfur oxidation by the O₃ oxidation mechanism from 16% to 39 and 46%, respectively, while the relative contribution of halogen oxidation and H₂O₂ oxidation dropped from 38% for each to 20–23% and 27–32%, respectively (numbers are mean values integrated over the depth of the MBL). Still higher 200% added biogenic alkalinity (under cloud-free conditions) indicates that O₃ oxidation in sea-salt aerosol water may contribute 75–80% to total sulfur oxidation under typical cloud-free RMBL conditions.

4. Conclusions

[49] The primary conclusion from this study is that O₃ oxidation in sea-salt aerosol water produces significantly more NSS in the remote MBL (RMBL) than that limited by seawater nonbiogenic alkalinity. We propose that the alkalinity supplied by Ca⁺⁺ from calcareous plankton debris, under typical near-surface RMBL wind speed and upwind surface waters primary productivity conditions, is sufficient to increase the NSS produced by O₃ oxidation in the sea-salt aerosol water of coarse, supermicron ambient diameter sea-salt aerosols by an estimated ~1.5–2 nmol m⁻³ beyond the <=0.5 nmol NSS m⁻³ produced when only seawater nonbiogenic alkalinity prevails. The relatively clear sky conditions and high wind speed aerosol data set collected

at Baring Head, a unique RMBL data set (Table 1, clear sky southerly), shows that quite substantial NSS concentrations may be produced in coarse aerosol sea-salt aerosol water when precipitation and cloud processing do not impede the accumulation of excess Ca⁺⁺ from calcareous plankton debris in coarse aerosol sea-salt aerosol water. The 30 nmol m⁻³ excess Ca⁺⁺, Ca⁺⁺Excess in Table 1, introduced >200 times more alkalinity to the sea-salt aerosol water of coarse aerosols in this clear sky southerly data set than did nonbiogenic seawater alkalinity. More than 8 nmol NSS m⁻³ was produced in coarse aerosols by O₃ oxidation in sea-salt aerosol water during clear sky southerly conditions at Baring Head. These are significantly greater levels of NSS than can be expected under typical wind speeds since all data in Table 1 were obtained with ~11 m s⁻¹ wind speeds and an upwind ocean surface layer annual primary productivity of 350–400 gC m⁻² versus typical open ocean surface layer annual primary productivity of ~130 gC m⁻².

[50] Ozone oxidation in the sea-salt aerosol water of coarse aerosols was sustained by excess Ca⁺⁺, again very likely from calcareous plankton debris, during the ACE-Asia Hawaii to Japan transit of the RV *Brown* such that 1.8 ± 0.3 nmol m⁻³ additional NSS was produced during more typical RMBL conditions than were observed at Baring Head. Thus the sum of seawater biogenic and non-biogenic alkalinity may be expected to produce on the order of 2 nmol NSS m⁻³ by O₃ oxidation in sea-salt aerosol water under more typical RMBL conditions, sufficiently large to be the sink for a substantial fraction of the gaseous sulfur emitted from remote areas of the global oceans. In high wind speed areas of the RMBL and/or downwind of highly productive ocean surface waters regions, such as the subtropical front region upwind of Baring Head, the NSS due to O₃ oxidation in high alkalinity sea-salt aerosol water may be the atmospheric endpoint for all of the gaseous sulfur emitted from these surface waters. O₃ oxidation in the sea-salt aerosol water of, mainly, coarse sea-salt aerosols then provides for a rapid NSS return to surface waters through dry deposition of these coarse aerosols.

[51] The NSS associated with coarse, ≥1 μm ambient diameter sea-salt aerosols has a dry removal rate of about 1 cm s⁻¹ [Slinn and Slinn, 1980; Sievering, 1984], under typical ~6 m s⁻¹ RMBL wind speed conditions. Thus a large fraction of ocean-derived dimethylsulfide (DMS), once converted to SO₂, is further converted to NSS in coarse sea-salt aerosols and, finally, dry deposited back to the ocean's surface waters.

[52] The conversion of SO₂ to sulfate aerosols can occur via two broad mechanisms. Homogeneous nucleation results in new particles via the condensation of SO₂ in the gas phase to sulfate aerosols. Heterogeneous conversion, such as O₃ oxidation, involves SO₂ gas reacting at the surface of an existing aerosol and, while this process results in a change in chemistry of the original aerosol, it does not result in a new particle. Typically, in the RMBL, sea-salt represents a significant sink for SO₂ and indicates that heterogeneous conversion is the dominant process since it is energetically more favorable than homogeneous nucleation [Twomey, 1977]. DMS derived SO₂ becomes effectively "locked up" in sea-salt aerosols, which renders it unavailable to participate in new particle formation (through nucleation), and limits its role in generating cloud conden-

sation nuclei. The feedback between greenhouse warming, oceanic DMS emissions, and sulfate cloud condensation nuclei and cloud albedo (the often referred to CLAW hypothesis [Charlson *et al.*, 1987]) may be sharply reduced by rapid sulfur return to the ocean's surface waters induced by O₃ oxidation in sea-salt aerosol water. While there has been debate over the biological role of DMS(P), it is intriguing that the coccolithophores are both efficient producers of the DMSP precursor of biogenic NSS and of calcareous debris which provides a powerful mechanism for preventing new particle production by the DMS by-product.

[53] A secondary conclusion relates to current global/ocean modeling. *Barrie et al.* [2001] showed in COSAM that on average, models overpredict SO₂ mixing ratios by twofold, and more. Both *Barrie et al.* [2001] and *Kasibhatla et al.* [1997] also indicate that models, often, tend to underpredict sulfate. The enhanced O₃ oxidation due to biogenically derived alkalinity in sea-salt aerosols markedly reduces SO₂ in the RMBL and, slightly, increases the sulfate in coarse aerosols (1.5–2 nmol NSS m⁻³). This heterogeneous conversion process needs to be explicitly included in global/ocean modeling to better align modeled and observed atmospheric sulfur data. (It should be noted that HOCl and HOBr oxidation in sea-salt aerosol water also reduces the SO₂ present in the RMBL.)

[54] Biogenically (Ca⁺⁺Excess) enhanced O₃ oxidation may also contribute to the generation of NSS in fine and very fine aerosols, given the clear sky southerly results as well as the observation that >0.15 μm diameter aerosol sulfur in the RMBL of the Weddell Sea and the Southern Ocean is dominated by CaSO₄ [Artaxo *et al.*, 1992]. Finally, the role of O₃ oxidation, especially in productive (and variable productivity) regions of the global oceans where calcareous plankton debris may be expected to enhance alkalinity, needs to be fully assessed in future experimental work such as that to be undertaken during the Australian/New Zealand Surface Ocean-Lower Atmosphere Study (SOLAS-ANZ) of March–May, 2004.

[55] **Acknowledgments.** We would like to thank Ian Boyd, Andrew Marriner and Jerram Robinson of the National Institute of Water and Air Research (NIWA) of New Zealand for their assistance with field work and lab analyses that was integral to the present effort. We also thank: Brian Lerner and Eric Sievering of the Univ. of Colorado for their assistance with the set up of equipment and the establishment of field protocols at the Baring Head site; Roland von Glasow of Heidelberg Univ. for modeling analyses specific to our Baring Head data critique; and Jim Anderson of Arizona State Univ. for individual particle analysis of Baring Head aerosols. This research was funded by NSF's Geosciences Directorate, Atmospheric Sciences Division grant ATM-980874 and New Zealand FRST research contract CO1X0204 "Drivers and Mitigation of Global Change". It is a contribution to the International Global Atmospheric Chemistry (IGAC) project of the International Geosphere-Biosphere Program.

References

- Allen, A., A. Dick, and B. Davison (1997), Sources of atmospheric MSA, NSS sulfate, and related species over the temperate South Pacific, *Atmos. Environ.*, *31*, 191–205.
- Artaxo, P., M. Rabello, W. Maenhaut, and R. van Grieken (1992), Trace elements and individual particle analysis of atmospheric aerosols over the Weddell Sea, *Tellus, Ser. B*, *44*, 318–334.
- Ayers, G., and J. Gras (1983), The concentration of ammonia in Southern Ocean air, *J. Geophys. Res.*, *88*, 10,655–10,659.
- Barrie, L. A., et al. (2001), A comparison of large scale atmospheric sulphate aerosol models (COSAM), *Tellus, Ser. B*, *53*, 615–642.
- Behrenfeld, M., and P. Falkowski (1997), Photosynthetic rates derived from satellite-based chlorophyll concentrations, *Limnol. Oceanogr.*, *42*, 1–20.

- Berner, A., C. Lurger, F. Pohl, and P. Wagner (1979), The size distribution of the urban aerosol in Vienna, *Sci. Total Environ.*, *13*, 245–261.
- Bradford-Grieve, J., F. Chang, M. Gall, S. Pickmere, and F. Richards (1997), Size-fractionated phytoplankton standing stocks and primary productivity during the austral winter and spring 1993 in the Subtropical Convergence region near New Zealand, *J. Mar. Freshwater Res.*, *31*, 201–224.
- Brown, C., and J. Yoder (1994), Coccolithophorid blooms in the global oceans, *J. Geophys. Res.*, *99*, 7467–7482.
- Caine, J. M., G. P. Ayers, H. Sievering, R. W. Gillett, and M. A. Hooper (1999), The use of magnesium as a marker for sea salt at Cape Grim, in *Baseline Atmospheric Program—1996*, edited by J. L. Gras et al., pp. 7–14, Bur. of Meteorol., Melbourne, Australia.
- Cattell, F., W. Scott, and D. du Cros (1977), Chemical composition of aerosol particles >1 μm diameter in the vicinity of Tasmania, *J. Geophys. Res.*, *82*, 3457–3462.
- Chameides, W., and A. Stelson (1992), Aqueous-phase chemical processes in deliquescent seasalt aerosols, *J. Geophys. Res.*, *97*, 20,565–20,580.
- Chang, F., J. Zeldis, M. Gall, and J. Hall (2003), Seasonal and spatial variation of phytoplankton assemblages, biomass and cell size from the spring to summer across the northeastern New Zealand continental shelf, *J. Plankton Res.*, *25*, 737–758.
- Charlson, R., J. Lovelock, M. Andreae, and S. Warren (1987), Oceanic phytoplankton, atmospheric sulfur, cloud albedo, and climate, *Nature*, *326*, 655–661.
- DeBruyn, W., M. Harvey, J. Caine, and E. Saltzman (2002), DMS and SO₂ at Baring Head, NZ: Implications for SO₂ yield from DMS, *J. Atmos. Chem.*, *41*, 189–209.
- Dorling, S. R., T. D. Davies, and C. E. Pierce (1992), Cluster analysis: A technique for estimating the synoptic meteorological controls on air and precipitation chemistry, *Atmos. Environ., Part A*, *26*, 2575–2582.
- Duce, R., and E. Hoffman (1976), Chemical fractionation at the air/sea interface, *Annu. Rev. Earth Planet. Sci.*, *3*, 187–228.
- Findlay, C., and J. Giraudeau (2000), Extant calcareous nannoplankton in the Australian sector of the Southern Ocean, *Mar. Micropaleontol.*, *40*, 417–439.
- Gomez, A. J. (Ed.) (1996), *Baring Head Atmospheric Data Summary, NIWA Sci. Technol. Ser. 39*, Natl. Inst. of Water and Atmos. Res., Wellington, New Zealand.
- Gordon, N. (1986), Computer derived air trajectories, *Rep. 22*, N. Z. Meteorol. Serv., Wellington.
- Gravenhorst, G. (1978), Sulfate over the North Atlantic, *Atmos. Environ.*, *2*, 707–713.
- Gurciullo, C., B. Lerner, H. Sievering, and S. Pandis (1999), Heterogeneous sulfate production in the marine environment, *J. Geophys. Res.*, *104*, 21,719–21,731.
- Harvey, M. J., S. M. Turner, J. E. Robinson, J. Hall, and P. W. Boyd (2002), Production of DMS around the sub-tropical front and in the iron limited Southern Ocean, *Eos Trans. AGU*, *83*(22), West. Pac. Geophys. Meet., Abstract A41A-02.
- Henricks, S., and P. Williams (1985), Dissolved and particulate amino acids and carbohydrates in the sea surface microlayer, *Mar. Chem.*, *17*, 141–163.
- Hoppel, W., G. Frick, J. Fitzgerald, and B. Wattle (1994), A cloud chamber study of the effect that clouds have on the aerosol size distribution, *Aerosol Sci. Technol.*, *20*, 1–30.
- Junge, C. E. (1972), Our knowledge of the physico-chemistry of aerosols in the undisturbed marine environment, *J. Geophys. Res.*, *77*, 5183–5200.
- Kasibhatla, P., W. L. Chameides, and J. St. John (1997), A three-dimensional global model investigation of seasonal variations in the atmospheric burden of anthropogenic sulfate aerosols, *J. Geophys. Res.*, *102*, 3737–3749.
- Keene, W., R. Sander, A. Pszenny, R. Vogt, and P. Crutzen (1998), Aerosol pH in the marine boundary layer: A review, *J. Aerosol Sci.*, *29*, 339–356.
- Kleinbaum, D., L. Kupper, K. Muller, and A. Nizam (1998), *Applied Regression Analysis and Other Multivariable Methods*, 775 pp., Duxbury, New York.
- MacIntyre, F. (1974), Chemical fractionation and sea surface processes, *Sea*, *5*, 245–299.
- Maenhaut, W., A. Selen, and J. Winchester (1983), Characterization of the atmospheric aerosol over the eastern equatorial Pacific, *J. Geophys. Res.*, *88*, 5353–5364.
- Millero, F. J. (1974), The physical chemistry of seawater, *Annu. Rev. Earth Plan. Sci.*, *2*, 101–150.
- Moore, J., and M. Abbott (2000), Chlorophyll distributions and primary production in the Southern Ocean, *J. Geophys. Res.*, *105*, 28,709–28,722.
- O'Dowd, C., M. Smith, and J. Lowe (1997), Marine aerosol, seasalt, and the marine sulphur cycle, *Atmos. Environ.*, *31*, 73–80.
- Prospero, J. M., and D. Savoie (1993), AEROCE scientific results 1988–1992, *RSMAS-883*, Rosenthal Sch. of Mar. and Atmos. Sci., Univ. of Miami, Miami, Fla.
- Quinn, P. K., et al. (2004), Aerosol optical properties measured on board the *Ronald H. Brown* during ACE-Asia as a function of aerosol chemical composition and source region, *J. Geophys. Res.*, *109*, D19S01, doi:10.1029/2003JD004010.
- Schlesinger, W. (1997), *Biogeochemistry: Global Change*, p. 302, Academic, San Diego, Calif.
- Sievering, H. (1984), Small particle dry deposition on natural waters: Modeling uncertainty, *J. Geophys. Res.*, *89*, 9679–9681.
- Sievering, H., G. Ennis, E. Gorman, and C. Nagamoto (1990), Heterogeneous sulfur conversion in sea salt aerosol particles, *Global Biogeochem. Cycles*, *4*, 395–406.
- Sievering, J., J. Boatman, J. Galloway, W. Keene, Y. Kim, and M. Luria (1991), Heterogeneous sulfur conversion in seasalt aerosol particles: The role of aerosol water content and size distribution, *Atmos. Environ., Part A*, *25*, 1479–1487.
- Sievering, H., J. Boatman, E. Gorman, Y. Kim, L. Anderson, G. Ennis, M. Luria, and S. Pandis (1992), Removal of sulfur from the marine boundary layer by ozone oxidation in seasalt aerosols, *Nature*, *360*, 571–574.
- Sievering, H., J. Boatman, E. Gorman, T. Ley, and Y. Kim (1995), Ozone oxidation in of sulfur in seasalt particles during the Azores Marine Aerosol and Gas Exchange Experiment, *J. Geophys. Res.*, *100*, 23,075–23,081.
- Sievering, H., B. Lerner, J. Slavich, and J. Caine (1999), O₃ oxidation of SO₂ in seasalt aerosol water: Size distribution of NSS during the First ACE Experiment, *J. Geophys. Res.*, *104*, 21,707–21,717.
- Slinn, S., and W. Slinn (1980), Predictions for particle deposition on natural waters, *Atmos. Environ.*, *14*, 1013–1016.
- Tseng, R., R. Skop, and J. Brown (1992), Sea-to-air transfer of surface-active organic compounds by bursting bubbles, *J. Geophys. Res.*, *97*, 52–58.
- Twomey, S. (1977), *Atmospheric Aerosols*, 302 pp., Elsevier Sci., New York.
- Uddstrom, M., W. Gray, R. Murphy, N. Oien, and T. Murray (1999), A Bayesian cloud mask for sea surface temperature retrieval, *J. Atmos. Oceanic Technol.*, *16*, 117–132.
- Uddstrom, M., J. McGregor, W. Gray, and J. Kidson (2001), A high-resolution analysis of cloud amount and type over complex topography, *J. Appl. Meteorol.*, *40*, 16–33.
- Vogt, R., P. Crutzen, and R. Sander (1996), A mechanism for halogen release from seasalt aerosol in the remote marine boundary layer, *Nature*, *383*, 327–330.
- von Glasow, R., and P. Crutzen (2004), Model study of multiphase DMS oxidation with a focus on halogens, *Atmos. Chem. Phys.*, *3*, 6733–6777.
- von Glasow, R., R. Sander, A. Bott, and P. Crutzen (2002), Modeling halogen chemistry in the marine boundary layer: 2. Interactions with sulfur and the cloud-covered MBL, *J. Geophys. Res.*, *107*(D17), 4323, doi:10.1029/2001JD000943.
- Warneck, P. (1988), *Chemistry of the Natural Atmosphere*, 757 pp., Academic, San Diego, Calif.
- Wratt, D., et al. (1996), The New Zealand Alps experiment, *Bull. Am. Meteorol. Soc.*, *77*, 683–692.
- Wylie, D. J., and S. J. de Mora (1996), Atmospheric dimethylsulfide and sulfur species in aerosol and rainwater at coastal site in New Zealand, *J. Geophys. Res.*, *101*, 21,041–21,049.
- Xuan, J., and I. Sokolik (2002), Characterization of sources and emission rates of mineral dust in northern China, *Atmos. Environ.*, *36*, 4863–4876.

J. Caine, Cape Grim Baseline Air Pollution Station, Tasmania 7330, Australia.

M. Harvey, J. McGregor, and S. Nichol, National Institute of Water and Atmospheric Research, Wellington, New Zealand.

P. Quinn, Pacific Marine Environmental Laboratory, National Oceanic and Atmospheric Administration, 7600 Sand Point Way NE, Seattle, WA 98115, USA.

H. Sievering, Department of Geography and Environmental Science, University of Colorado, CB 172, PO 173364, Denver, CO 80217, USA. (hsieveri@carbon.cudenver.edu)